Numerically Efficient Optimal Design Of Cosine-Modulated Filter Banks With Peak-Constrained Least-Squares Behavior

Miguel B. Furtado, Jr., *Student Member, IEEE*, Paulo S. R. Diniz, *Fellow, IEEE*, and Sergio L. Netto, *Senior Member, IEEE*

***Abstract*—Several current applications related to signal compression and representation and high-speed transmission require very selective filter banks/transmultiplexers. A possible solution is to employ the cosine-modulated filter banks/transmultiplexers (CMFBTs) where the prototype filters satisfy demanding constraints with respect to both the total stopband energy and maximum stopband ripple. This work proposes an efficient procedure to design nearly-perfect reconstruction CMFBT prototype filters with peak-constrained least-squares characteristics using a modified weighted least-squares algorithm. Substantial flexibility is added in the design of the magnitude response of the prototype filter, ranging from minimum stopband energy to minimum stopband ripple, which may be required in many applications. Some constraints are imposed to the CMFBTs in order to control the direct transfer and aliasing distortion functions, related to the intercarrier and intersymbol interferences. Algebraic simplifications are also provided on the overall objective function and associated constraints, leading to substantial reduction on the computational burden of the optimization process. The procedure is proven to be very powerful in designing CMFBT systems satisfying multiple constraints as indicated by numerical examples.**

***Index Terms*—Cosine-modulated filter banks (CMFBs), transmultiplexers.**

I. Introduction

FILTER banks and transmultiplexers consisting of very selective subfilters have found applications in compression and representation of some specific signals [18], and in high-speed transmission over dispersive channels [20], [21]. In particular, communication systems based on multicarrier modulation have been used in several applications due to the ability of splitting the transmitted signal into M almost orthogonal subbands, which can be equalized separately [2]. Most of these systems are based on discrete multitone modulation (DMT) [4], [24] or discrete wavelet multitone modulation (DWMT) [6], [21], where a transmultiplexer configuration is used. As main examples of DMT systems are the ones based on the discrete Fourier transform (DFT) and an inverse DFT (IDFT) transforms, which find application in digital video and audio broadcasting and the recently proposed principal component filter bank (PCFB) [24], among others. As an example of a DWMT system is the cosine-modulated filter bank (CMFB) which was proposed in the design of very high rate digital subscriber line (VDSL) modems [25]. The DFT-based multicarrier modulator presents poor frequency separation among its subbands, whereas the DWMT may present very selective subchannels, depending on the choice of the bank structure [21]. The PCFB may be an optimal filter bank in the sense of maximizing the bit rate for a given constrained transmitted power. The cosine-modulated filter bank/transmultiplexer (CMFBT) is an attractive choice for the analysis and synthesis filters of a DWMT multichannel system due to its simplicity and fast implementation [23]. Also, subband coding based on filter banks has become a very popular tool for signal compression, due to the inherent spectral analysis performed by their orthogonal subfilters. Both transmultiplexer and filter bank are known as multirate systems, where in the transmultiplexer structure, the analysis and synthesis filters are placed in reverse order with respect to the filter bank. In this way, the figures of merit of both structures are closely related [25], as will also be explored in the present paper.

The filter design approach minimizing the stopband energy is called least squares (LS), whereas the one minimizing the maximum stopband ripple is usually referred to as the peak-constrained or minimax method. This paper presents a numerical method for designing nearly perfect reconstruction (NPR) CMFBTs satisfying a tradeoff between both LS and minimax objectives, where solutions ranging from minimum stopband energy to minimum stopband ripple are possible. The result is the so-called peak-constrained LS (PCLS) solution. The proposed method is based on a modified version of the weighted LS (WLS) algorithm [14] known as the WLS-Chebyshev algorithm [7], but substantially improved. The main contribution is the ability of optimizing an objective function that combines both stopband measurements (energy and maximum ripple) subject to nonlinear constraints. The result is a very flexible design procedure for optimal CMFBTs in the sense of achieving the nonlinear constraints with minimized stopband energy and ripple. Numerical efficiency of the design procedure is also established by taking advantage of a series of algebraic simplifications in the overall objective function and associated constraints as provided in this paper. It is worth mentioning that the PCLS is a criterion introduced in [1] which qualifies a given design solution, whereas the WLS-Chebyshev is an algorithm used to achieve the PCLS solution. The algorithm proposed in this article is a modified version of the WLS-Chebyshev.

Manuscript received August 5, 2003; revised March 23, 2004. This paper was recommended by Associate Editor W.-P. Zhu.

The authors are with the Electrical Engineering Program at Federal University of Rio de Janeiro, Rio de Janeiro, RJ 21945-970, Brazil (e-mail: furtado@lps.ufrj.br; diniz@lps.ufrj.br; sergioln@lps.ufrj.br).

Digital Object Identifier 10.1109/TCSI.2004.842879

The remaining of the paper is organized as follows. Section II, presents an introduction to the CMFBT structures. In Section III the optimized design of CMFBTs is discussed based on the PCLS criterion. Section IV presents the WLS-Chebyshev algorithm as an efficient and powerful alternative to determine the PCLS solution for practical CMFBTs. In Section V, numerically efficient forms of the PCLS objective-function gradient vector and design constraints are provided in order to generate a simplified optimization procedure. Section VI presents some CMFBT designs obtained using the proposed WLS-Chebyshev procedure utilizing a numerically efficient routine. At the end of the paper, an Appendix provides all algebraic development related to the simplifications included in Section V.

II. Cosine-Modulated Filter Banks and Transmultiplexers

CMFBTs are multirate structures that rely on the design of a single prototype filter for both analysis and synthesis banks, which will be modulated to generate all subfilters of the filter bank. Moreover, there is a fast implementation for the CMFBTs based on the DCT-IV transform [8], [23], and, as a consequence, they have been used in several applications like DSL modems [6], [20], [25] and subband coding [18].

Assuming that the prototype filter has an impulse response $h_p(n)$ of order N_p, its transfer function is expressed as

$$H_p(z) = \boldsymbol{h}_p^T \boldsymbol{d}(z) \tag{1}$$

$$\boldsymbol{h}_p = [\, h_p(0) \quad h_p(1) \quad \dots \quad h_p(N_p)\,]^T \tag{2}$$

$$\boldsymbol{d}(z) = [\, 1 \quad z^{-1} \quad \dots \quad z^{-N_p}\,]^T. \tag{3}$$

The fast implementation of the CMFBT presented in [23] requires an order $N_p = (2KM - 1)$ for the prototype filter, with K being a positive integer, which determines the length of the $2M$ polyphase components of $H_p(z)$.

The analysis and synthesis subfilters are cosine-modulated versions of the prototype filter, which can be described by

$$H_m(z) = \alpha_m \beta_m^{N_p/2} H_p(z\beta_m) + \alpha_m^* \beta_m^{-N_p/2} H_p(z\beta_m^*) \tag{4}$$

$$F_m(z) = \alpha_m^* \beta_m^{N_p/2} H_p(z\beta_m) + \alpha_m \beta_m^{-N_p/2} H_p(z\beta_m^*) \tag{5}$$

where $\alpha_m = e^{j(-1)^m(\pi/4)}$, $\beta_m = e^{-j(2m+1)(\pi/2M)}$, and * denotes the complex conjugate operator.

Fig. 1 shows the block diagram of the filter bank described above, with the input–output relation being described by [23]

$$\hat{Y}(z) = \frac{1}{M}\left[T_0(z)Y(z) + \sum_{i=1}^{M-1} T_i(z)Y(ze^{(j2\pi i/M)})\right]. \tag{6}$$

The first term in (6), $T_0(z)$, is the direct transfer function and must be the only term in an alias-free design, which includes the PR filter bank as a particular case. The second term, involving all other $T_i(z)$, contains the aliasing transfer functions, which quantify the influences in a given band from all other bands. These terms are expressed by

$$T_i(z) = \sum_{m=0}^{M-1} F_m(z) H_m(ze^{(-j2\pi i/M)}) \qquad i = 0, 1, \dots, M-1. \tag{7}$$

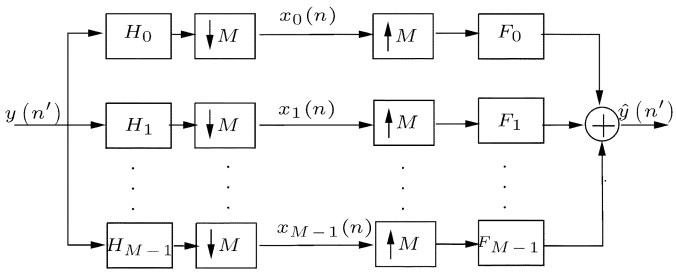

Fig. 1. M-channel maximally decimated filter bank.

The maximally decimated M-channel transmultiplexer (TMUX) system is a multirate system where the positions of the analysis and synthesis banks are reversed to form a system with M input/output channels, as depicted in Fig. 2 [9], [23]. This structure interpolates and filters each input signal, adding the resulting signals on each branch to form a single signal for transmission over a given channel C. At the receiver, the signal is then split back into M-channels to generate the desired M outputs. The design problem of such a system can be simplified by assuming that the channel response is ideal $(C \equiv 1)$ or a pure delay. Then, in the PR case, each output signal is identical to its equivalent input, whereas in the NPR, small interferences among the subchannels are present. In order to keep the PR/NPR property of the bank, a small delay z^{-d} may be inserted in the TMUX system before the demultiplexer block [23].

The general relation that describes the transfer functions of the TMUX system is given by [9]

$$\hat{\boldsymbol{x}}(z^M) = \frac{1}{M}\check{\boldsymbol{T}}(z^M)\boldsymbol{x}(z^M) \tag{8}$$

where

$$\hat{\boldsymbol{x}}(z) = [\, \hat{X}_0(z) \quad \hat{X}_1(z) \quad \dots \quad \hat{X}_{M-1}(z)\,]^T \tag{9}$$

$$\boldsymbol{x}(z) = [\, X_0(z) \quad X_1(z) \quad \dots \quad X_{M-1}(z)\,]^T \tag{10}$$

and

$$[\check{\boldsymbol{T}}(z^M)]_{ab} = \sum_{m=0}^{M-1} H_a(ze^{-(j2\pi m/M)}) F_b(ze^{-(j2\pi m/M)}) \tag{11}$$

for $a, b = 0, 1, \dots, (M-1)$. The matrix $\check{\boldsymbol{T}}(z^M)$ is the so-called transfer matrix whose elements, $[\check{\boldsymbol{T}}(z^M)]_{ab}$, represent the transfer function between the interpolated input a and the interpolated output b. Thus, the main diagonal entries of this matrix, $[\check{\boldsymbol{T}}(z^M)]_{aa}$, represent the transfer functions of each subchannel, and the remaining terms account for the crosstalk between two different subchannels. In the NPR case, no restrictions apply to the transfer function matrix, whereas in the PR case, the crosstalk terms must be zero and the diagonal terms become simple delays [25].

In a TMUX system, one would be interested in estimating the total intersymbol interference (ISI) and intercarrier interference (ICI) figures of merit, which are given by [3]

$$\text{ISI} = \max_a \left\{ \sum_n [\delta(n-d) - \check{t}_{aa}(n)]^2 \right\} \tag{12}$$

$$\text{ICI} = \max_{a,\omega} \left\{ \sum_{b=0, b\neq a}^{M-1} |[\check{\boldsymbol{T}}(e^{j\omega})]_{ab}|^2 \right\} \tag{13}$$

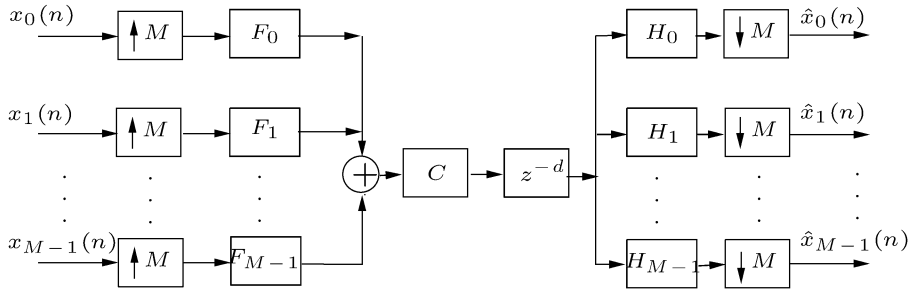

Fig. 2. M-channel maximally decimated TMUX system.

where $\delta(n)$ is the ideal impulse, d is a proper delay, $\check{t}_{aa}(n)$ is the impulse response for the ath subchannel, and the term $[\check{\boldsymbol{T}}(e^{j\omega})]_{ab}$ is the crosstalk between the ath and bth subchannels, whose expression is given by (11).

In the design of filter banks, some constraints are imposed by the nature of the problem, such as the maximum overall amplitude distortion, d_1, and aliasing interference, d_2, given by

$$d_1 = \max_{\omega} \left\{ \left| |T_0(e^{j\omega})| - 1 \right| \right\} \tag{14}$$

$$d_2 = \max_{i,\omega} \left\{ |T_i(e^{j\omega})| \right\}, \qquad i = 1, \ldots, N_c \tag{15}$$

where $N_c = \lfloor M/2 \rfloor$ is the total number of constraints,[1] with the operator $\lfloor x \rfloor$ denoting the integer part of x.

As verified in [23], the ISI and ICI in a TMUX system are closely related to the overall amplitude distortion and the aliasing interference in a filter bank, respectively. Therefore, filter banks with reduced direct and aliasing transfer distortions and selective frequency response are TMUX systems with reduced ISI and ICI with great spectral containment and vice-versa.

III. CMFBT Optimization Problem

In the design of digital filters, it is common to find applications requiring the magnitude response of the resulting filter error function to be minimized in an LS or minimax sense. In some cases, the constraints imposed by the problem automatically determine the passband gain, which, consequently, is not taken into account in the original objective function. In this way, the LS and minimax objective functions for the design of a low-pass filter can be defined as

$$E_{\mathfrak{p}}(\boldsymbol{h}_p) = \left(\int_{\omega_s}^{\pi} |H_p(e^{j\omega})|^{\mathfrak{p}} d\omega \right)^{(\mathfrak{q}/\mathfrak{p})} \tag{16}$$

with $\mathfrak{p} = 2$ ($\mathfrak{q} = 2$) and $\mathfrak{p} = \infty$ ($\mathfrak{q} = 1$), respectively, where $H_p(e^{j\omega})$ is the frequency response of the prototype filter and ω_s is its stopband edge frequency. For finite-impulse response (FIR) filters, the E_2 objective function can be optimized analytically, as described, for instance in [8], [22], while the minimax E_∞ optimization problem can be solved using the Parks–McClellan algorithm [19].

Traditional filter design algorithms [8], however, are not suitable to solve the general CMFBT optimization problem due to the required nonlinear constraints. In such cases, the problem of finding an optimized solution can be solved with a modified objective function $\hat{F}(\boldsymbol{h}_p)$, that combines the original objective function $E_{\mathfrak{p}}(\boldsymbol{h}_p)$ with a weighted set of constraints, such that

$$\hat{F}(\boldsymbol{h}_p) = E_{\mathfrak{p}}(\boldsymbol{h}_p) + \boldsymbol{\lambda}^T \boldsymbol{c}(\boldsymbol{h}_p) \tag{17}$$

where $\boldsymbol{h}_p$ is as given in (2), considering only $N_p = KM$ coefficients due to the linear-phase property of the prototype filter, $\boldsymbol{\lambda}$ is the vector of constraint weights, and $\boldsymbol{c}(\boldsymbol{h}_p)$ is the vector of constraints, that is

$$\boldsymbol{\lambda} = [\, \lambda_0 \quad \lambda_1 \quad \ldots \quad \lambda_{N_c} \,]^T \tag{18}$$

$$\boldsymbol{c}(\boldsymbol{h}_p) = [\, c_0(\boldsymbol{h}_p) \quad c_1(\boldsymbol{h}_p) \quad \ldots \quad c_{N_c}(\boldsymbol{h}_p) \,]^T \tag{19}$$

where $N_c = \lfloor M/2 \rfloor$, as stated before.

The minimization of $E_{\mathfrak{p}}(\boldsymbol{h}_p)$ in (17) will be performed using a modified WLS-Chebyshev introduced in Section IV in order to achieve the PCLS solution. The minimization problem can be solved using quadratic programming (QP) algorithms [16], which whenever possible require the first and second derivatives of $E_{\mathfrak{p}}(\boldsymbol{h}_p)$ to simplify its implementation and improve the performance. With the QP algorithms, the constraint weights are set by the designer. An alternative is to use a sequential QP (SQP) algorithm [16], which optimally sets the weights of the constraints based on the method of Lagrange multipliers with the Kuhn–Tucker conditions [16]. The problem of finding the optimum PCLS filter subject to nonlinear constraints was studied in [1], leading to a more complex design than the one proposed here. The design of PCLS 2-band filter banks can be found in [5]. A more generic treatment is found in [22], where a QP algorithm is used to optimize an objective function formulated similarly to (17). The spectral characteristics of the prototype filter is therein shaped with the LS or Minimax criterion. Another interesting technique is given in [17], where the prototype filter is constrained to be a spectral factorization of a Nyquist filter with LS characteristics. The result is a filter bank without direct transfer distortion. The use of a SQP algorithm was necessary to perform the optimization.

In practice, to control the aliasing distortion and the overall direct transfer of the filter bank, the following constraints are defined:

$$\hat{c}_0(\boldsymbol{h}_p, \omega_j) = \left| |T_0(e^{j\omega_j})| - 1 \right| - \delta_1 \leq 0 \tag{20}$$

$$\hat{c}_i(\boldsymbol{h}_p, \omega_j) = |T_i(e^{j\omega_j})| - \delta_2 \leq 0 \tag{21}$$

for $i = 1, 2, \ldots, N_c$ and $\omega_j \in [0, (\pi/M)]$, since the functions $T_i(e^{j\omega})$ are periodic with period (π/M), property which will

[1] Due to some symmetry in the aliasing terms, as stated in [22].

be discussed later in Section V. As observed, these constraints depend on ω_J, where by using more discrete points in the frequency grid leads to a more accurate design, but with higher computational complexity. As stated in [11], there should be at least $40K$ points in the frequency grid, leading to a total of about $N_c = 20KM$ constraints. The parameters δ_1 and δ_2 adjust the tightness of the constraints attainment.

In Section V, the connections between (20) and (21) with (19) will be made clear.

This article is totally dedicated to the design of NPR CMFBTs, which is in general more complicated than the PR design using power-complementary lattice sections [12] because the nonlinear constraints of the problem are inherently attained in the last one, but leads to more flexible implementations. Nevertheless, the NPR CMFBT has a fast implementation [8] but, unfortunately, the fastest implementation [18] available requires the use of PR prototypes.

IV. PCLS CMFBTS With Modified WLS-Chebyshev Approach

In this section, the WLS-Chebyshev algorithm is introduced along with the proposed modified WLS-Chebyshev aiming to achieve improved performance and to satisfy the nonlinear constraints imposed by the optimization problem inherent from the filter bank or TMUX design.

A. WLS-Chebyshev Algorithm

As given in [13] and [14], the solution of the minimax E_∞ problem can be approximated by successive weighted E_2 minimizations. An approximation of the weighted E_2 function in (16) is obtained by replacing the integral by a weighted summation at a discrete set of frequencies, leading to

$$E_2'(\boldsymbol{h}_p) = \sum_{\omega_i \in [\omega_s, \pi]} W_k^2(\omega_i) |H_p(e^{j\omega_i})|^2 \Delta_\omega \tag{22}$$

where $W_k(\omega_i)$ is the weighting function, at the kth iteration, with nonnegative samples, and Δ_ω is the given frequency grid interval.

To perform the PCLS optimization of an FIR filter, one can minimize (22) with the WLS-Chebyshev method described in [7], which is capable of achieving an excellent tradeoff between the LS and minimax norms. With the WLS-Chebyshev algorithm, the optimization procedure gradually modifies the objective function at each iteration by weighting each point in the frequency grid by the quadratic error between the desired (zero) and the actual responses in the stopband [7]. This is achieved by updating the weighting function at each iteration $k = 0, 1, \ldots, k_m$ in the form

$$W_{k+1}^2(\omega_i) = W_k^2(\omega_i) V_k(\omega_i) \tag{23}$$

$$V_k(\omega_i) = \begin{cases} B_k(\omega_i), & \omega_s \le \omega_i \le \omega_J \\ B_k(\omega_J), & \omega_J \le \omega_i \le \pi \end{cases} \tag{24}$$

with

$$B_k(\omega_i) = \frac{(\omega_i - \omega_I) E(\omega_{I+1}) + (\omega_{I+1} - \omega_i) E(\omega_I)}{(\omega_{I+1} - \omega_I)}, \quad \omega_I \le \omega_i \le \omega_{I+1} \tag{25}$$

and

$$E(\omega_i) = |H_p(e^{j\omega_i})|, \quad \omega_s \le \omega_i \le \pi \tag{26}$$

where the frequencies ω_I, arranged in increasing order, for $I = 1, 2, \ldots, J, \ldots, N_I$, correspond to the peaks of the error function $E(\omega_i)$ in the stopband, at the kth iteration. In this way, the function $B_k(\omega_i)$ becomes the envelope of $|H_p(e^{j\omega})|$ at that iteration. The parameter J uniquely characterizes the WLS-Chebyshev design, as it determines the frequency at which the prototype response switches from the minimax (equiripple) to the LS behavior. In particular, the LS and minimax designs correspond to $J = 1$ ($\omega_J = \omega_s$) and $J = N_I$ ($\omega_J = \pi$), respectively. As a result N_I is the index of the last peak of the error function, since the stopband edges are also considered as peaks [7]. Fig. 3 depicts the error function (dotted line) for a generic low-pass filter, along with its envelope $B_k(\omega)$ (dash-dotted line) and the modified envelope $V_k(\omega)$ (solid line), which is forced to be constant starting at frequency ω_J ($J = 5$ in the example).

B. Modified WLS-Chebyshev Algorithm

Now, a procedure for the design of PCLS prototype filters for CMFBTs based on the formulation of the modified objective function $\hat{F}(\boldsymbol{h}_p)$ is presented. Suppose that $\hat{F}(\boldsymbol{h}_p)$ takes into account the WLS objective function $E_2'(\boldsymbol{h}_p)$ and the nonlinear constraints of the problem, such that

$$\hat{F}(\boldsymbol{h}_p) = E_2'(\boldsymbol{h}_p) + \boldsymbol{\lambda}^T \boldsymbol{c}(\boldsymbol{h}_p). \tag{27}$$

The steps describing a smoothly convergent procedure are as follows:

1) Set the number of bands M and the overlapping factor K. Choose any LS behaved FIR prototype filter of length $2KM$ as the initial solution or, alternatively, use a PR prototype as described in [12], [22]. Set $k = 0$ (first iteration) and the parameter J that uniquely determines the WLS weighting function as

$$W_k^2(\omega_i) = \left(\frac{V_k(\omega_i)}{\bar{V}_k} \right)^{\theta_k} \tag{28}$$

with $V_k(\omega_i)$ given by (24), which must be evaluated over a dense frequency grid, with $S \approx 10N_p$ points, and where

$$\bar{V}_k = \frac{1}{S} \sum_{\omega_i} V_k(\omega_i) \quad \omega_i \in [\omega_s, \pi] \tag{29}$$

is the mean value of the envelope function evaluated at the kth iteration, and

$$\theta_k = \theta_{k-1}^{\psi} \tag{30}$$

is updated on each iteration by using the parameter ψ, starting with $\theta_0 = 1.5$. A good value for this parameter was found to be $\psi = 0.9$. Care should be taken to avoid that θ_k becomes very small. A good range for this parameter is given by [14] $1.2 \le \theta_k \le 2$, what means that θ_0 can even be greater than the value set by our procedure.

Choose a QP algorithm, setting up the constraint weights in the vector $\boldsymbol{\lambda}$ and providing the optimization

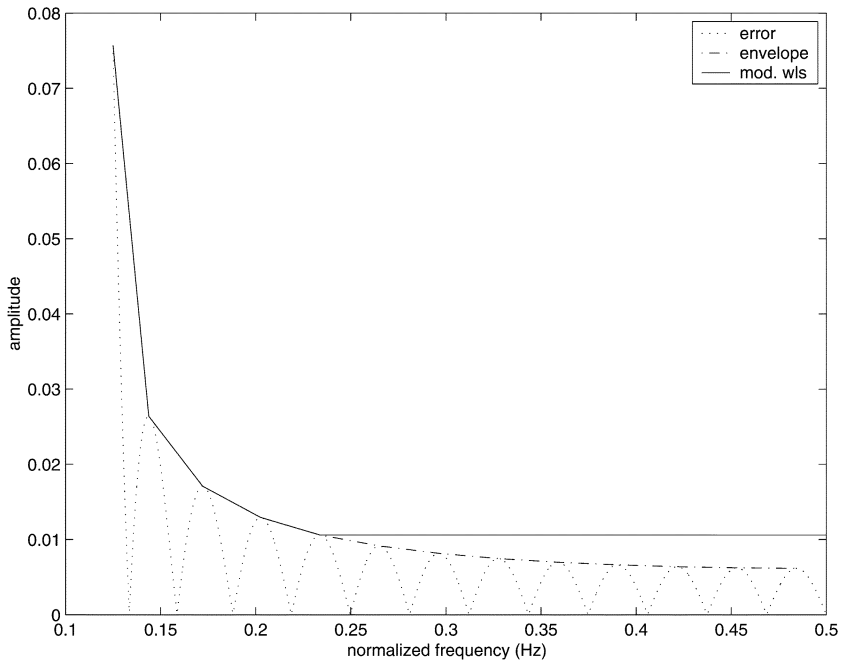

Fig. 3. Error function $E(\omega)$ (dotted line), and its derivations $B(\omega)$ (envelope, dash-dotted line) and $V(\omega)$ (solid line), for a generic low-pass filter.

algorithm with the function $\hat{F}(\boldsymbol{h}_p)$ and its derivatives. Optimize efficiently the prototype filter coefficients, keeping the WLS weighting function unaltered.

2) Set $k = k+1$. If $k = k_m$ is reached or any other tolerance criteria is met, stop. Otherwise, evaluate V_k and $\bar{V}_k$ as in (24) and (29) and update $W_k^2(\omega_i)$ as follows:

$$W_k^2(\omega_i) = \begin{cases} W_{k-1}^2(\omega_i)\left(\frac{V_k(\omega_i)}{\bar{V}_k}\right)^{\theta_k}, & \omega_i \in [\omega_s, \omega_J) \\ W_{k-1}^2(\omega_i)\left(\frac{\epsilon}{\bar{V}_k}\right)^{\theta_k}, & \omega_i \in [\omega_J, \pi] \end{cases} \tag{31}$$

where

$$\epsilon = \max_{\omega_J \le \omega_i \le \pi} \{V_k(\omega_i)\} \tag{32}$$

with θ_k updated using (30). With this new value of $W_k^2(\omega_i)$, evaluate $E_2'(\boldsymbol{h}_p)$ using (22). Then, optimize $\hat{F}(\boldsymbol{h}_p)$ in (27) efficiently using the QP algorithm, and return to Step 2). In general, $5 \le k_m \le 10$ is a good range for the number of iterations. If the choice is for the SQP algorithm, one must determine $E_2'(\boldsymbol{h}_p)$ and the constraints separately, along with their derivatives. It is worth mentioning that, when using a SQP-type algorithm, the vector of constraint weights $\boldsymbol{\lambda}$ is not used and the objective function reduces to

$$\hat{F}(\boldsymbol{h}_p) = E_2'(\boldsymbol{h}_p).$$

The proposed procedure uses a normalized weighting function [given by (28) and (31)], similar to the one proposed in [14], in order to ensure that the dynamic range of the weighting function are kept small. The main difference is that, here, the update is made in a smoother manner. Second, the weighting function has an extra parameter ϵ at the nonequiripple part of the stopband, avoiding that the weighting function becomes small at that region, ensuring that large ripples will never occur there.

V. Simplified Computation of Constraints and Gradient Vectors

A. Simplified Constraints

The large computational complexity to determine the constraints can be greatly reduced by defining the new constraints as [see (20) and (21)]

$$c_i(\boldsymbol{h}_p) = \sum_{\omega_j \in [0,(\pi/M)] \setminus \hat{c}_i > 0} \hat{c}_i^2(\boldsymbol{h}_p \omega_j) \tag{33}$$

which apparently have high computational complexity. However, all functions $T_i(e^{j\omega})$ can be evaluated using a simplified formulation, as given in Appendix, such that

$$T_i(e^{j\omega}) = e^{-j(\omega N_p + (\pi i/M))} A_{T_i}(\omega) \tag{34}$$

where

$$A_{T_i}(\omega) = 2Me^{j(\pi i/M)}\left[a_i(N_p) + 2\sum_{l=1}^{K-1} a_i(N_p - 2Ml)\cos[(2M\omega + \pi)l]\right] \tag{35}$$

with $a_i(n)$ given by

$$Z\left\{\left(e^{j(2\pi i n/M)} h_p(n)\right) * h_p(n)\right\} = \sum_{n=0}^{2N_p} a_i(n) z^{-n}. \tag{36}$$

On the right-hand side of (35), the variable ω is multiplying $2M$, what makes the trigonometric function $A_{T_i}(\omega)$ periodic with period (π/M). The proposed simplified formulation for the constraints enables a drastic reduction in the computational burden when compared with the original formulation, given in (7). For instance, assuming $K \gg 1$, the reduction factor is approximately $r \approx (1/2M^2)$ [11].

B. Simplified Gradient of $E_2'(\boldsymbol{h}_p)$

Given the objective function formulated in (22), and the definition of the modified constraints in (33), it is possible to de-

rive an equation for the partial derivatives of $\hat{F}(\boldsymbol{h_p})$ relative to the prototype filter coefficients, required by optimization algorithms based on quasi-Newton variants (e.g., the DFP and BFGS algorithms) [16]. In order to accomplish this, we can define

$$H_p(e^{j\omega}) = e^{(-j\omega N_p/2)} A_{h_p}(\omega) \tag{37}$$

where

$$A_{h_p}(\omega) = 2 \sum_{n=0}^{(N_p-1)/2} h_p(n) \cos\left[\omega\left(n - \frac{N_p}{2}\right)\right] \tag{38}$$

is the zero-phase frequency response of $H_p(e^{j\omega})$.

Rewriting (22) with the aid of (37), the following equation results:

$$E_2'(\boldsymbol{h}_p) = \sum_{\omega_i \in [\omega_s, \pi]} W^2(\omega_i) A_{h_p}^2(\omega_i) \Delta_\omega \tag{39}$$

and thus, its partial derivative with respect to $h_p(n)$, for $n = 0, 1, \ldots, (N_p - 1)/2$ (with N_p odd), becomes

$$\frac{\partial E_2'(\boldsymbol{h}_p)}{\partial h_p(n)} = 4\Delta_\omega \sum_{\omega_i} W^2(\omega_i) A_{h_p}(\omega_i) \cos\left[\omega_i\left(n - \frac{N_p}{2}\right)\right]. \tag{40}$$

C. Simplified Gradient of the Constraints

To determine the constraint derivatives, we can write, based on (33)

$$\frac{\partial c_i(\boldsymbol{h}_p)}{\partial h_p(n)} = 2 \sum_{\omega_j \in [0,(\pi/M)] \setminus \hat{c}_i > 0} \hat{c}_i(\boldsymbol{h}_p, \omega_j) \frac{\partial \hat{c}_i(\boldsymbol{h}_p, \omega_j)}{\partial h_p(n)} \tag{41}$$

with

$$\frac{\partial \hat{c}_i(\boldsymbol{h}_p, \omega_j)}{\partial h_p(n)} = \begin{cases} s(\hat{c}_i(\boldsymbol{h}_p, \omega_j)) s(A_{T_i(\omega_j)}) \frac{\partial A_{T_i}(\omega_j)}{\partial h_p(n)}, & i = 0 \\ s(A_{T_i}(\omega_j)) \frac{\partial A_{T_i}(\omega_j)}{\partial h_p(n)}, & i \neq 0 \end{cases} \tag{42}$$

where $s(x)$ is the sign of x and

$$\frac{\partial A_{T_i}(\omega_j)}{\partial h_p(n)} = 8M \cos\frac{\pi i(2n+1)}{M} \times \left[h_p(n) + \sum_{l=1}^{K-1} \left[h_p(n+2Ml) + h_p(n-2Ml)\right] \cos\left(2M\omega_j + \pi\right) l)\right] \tag{43}$$

with $h_p(n) = 0$, for $n < 0$ and $n > N_p$.

VI. Design Examples

The prototype filter for an M-band CMFBT can be specified by two cutoff frequencies

$$\omega_p = \frac{(1-\rho)\pi}{2M}; \quad \omega_s = \frac{(1+\rho)\pi}{2M} \tag{44}$$

where ω_p and ω_s are the passband and the stopband edge frequencies, respectively, and ρ is the so-called roll-off factor. It is desirable that $\omega_{3dB} \approx (\pi/2M)$, to keep the NPR property of the system. A quasi-Newton algorithm with line search, based on the BFGS algorithm [16], was applied in the optimization procedure described in Section IV, aiming to achieve improved performances with respect to E_2 and E_∞, for a given value of J and a constant overall amplitude distortion. The main idea is to analyze the behavior of the figures of merit d_2 and ICI when d_1 (or ISI) is made constant, for many possible tradeoffs between E_2 and E_∞, starting with the LS design (E_2 minimum and E_∞ maximum) and finishing with the minimax design (E_2 maximum and E_∞ minimum). All examples were simulated using Matlab®. Specifically for Example 3, where computational time was measured, the machine used was an AMD Athlon XP2600 with 516 MB of installed physical memory. At this point it is worth to reinforce that due to the nonlinearity of the constraints, the use of QP programming is necessary and not guaranteed to converge.

TABLE I
FIGURES OF MERIT FOR OPTIMIZED LS AND MINIMAX PROTOTYPE FILTERS IN EXAMPLE 1. IN ALL CASES $d_1 = 0.01$ AND ISI $= -43.0$ dB

Figures of Merit	LS	LS in [22]	Minimax
d_2 (dB)	-124.9	-125	-118.6
E_∞ (dB)	-112.4	-112.0	-123.4
E_2 (dB)	4×10^{-14}	4.5×10^{-14}	6.4×10^{-13}
ICI (dB)	-118.8	-118.8	-109.3

Example 1: The modified WLS procedure was applied in the design of a 32-band CMFBT, to demonstrate how the figures of merit of such system vary with the parameter J of the WLS-Chebyshev design. The specifications for this design were

$$\begin{cases} K = 8 \\ \rho = 1.0 \\ \delta_1 = 0.01 \\ \delta_2 \qquad \text{(as low as possible)} \end{cases} \tag{45}$$

which means that the constraint δ_1 must be attained and the constraint δ_2 was free, but the related aliasing distortion d_2 must be kept small.

It is worth mentioning that, in this example, the prototype filter order is given by $N_p = (2KM - 1) = 511$. Table I summarizes the results achieved by both LS ($J = 1, \omega_J = \omega_s$) and minimax ($J = N_I, \omega_J = \pi$) designs. There is also a comparison with the LS realization in [22], whose performance is measured based on the prototype filter coefficients kindly provided by the respective author. Clearly, both LS designs performed similarly. The LS case led to the lowest ICI and d_2 values, whereas the minimax to the highest levels of ICI and d_2. Fig. 4 depicts the main figures of merit as a function of J. Since d_2 is heavily dependent on the first neighboring subbands of the filter bank, and the equiripple part of the stopband occupies the bandwidth of the first neighboring bands, after a given value of J the figure of merit d_2 becomes practically constant. This behavior is clearly depicted in Fig. 4(a) for $J \geq 50$.

Example 2: This example demonstrates the behavior of the PCLS design for a fixed prototype filter length and different tradeoffs of stopband energy and maximum stopband ripple, and fixed levels of d_1 and d_2. The designed system was an 8-band CMFBT. The specifications were

$$\begin{cases} K = 8 \\ \rho = 1.0 \\ \delta_1 = 0.01 \\ \delta_2 = -126 \text{ (dB)} \end{cases} \tag{46}$$

meaning that both constraints on δ_1 and δ_2 must be attained, what made this example differ from the first one where the aliasing distortion d_2 was left free but desired to be small.

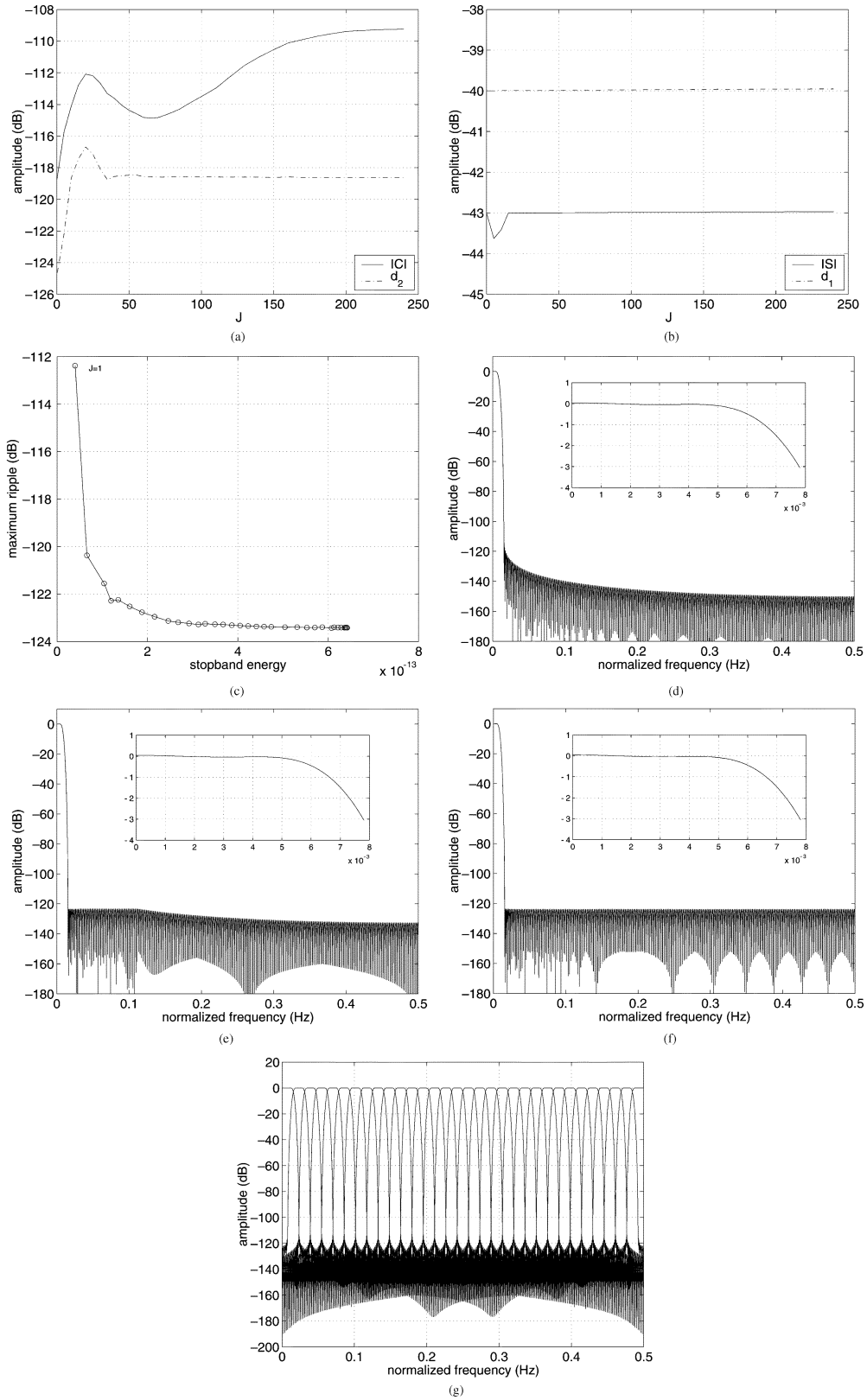

Fig. 4. Example 1 WLS-Chebyshev designs: (a) ICI (solid) and d_2 (dash-dot). (b) ISI (solid) and d_1 (dash-dot). (c) E_2/E_∞ tradeoff for different values of J. (d) Magnitude response of LS design ($J = 1$) and respective passband detail. (e) Magnitude response for $J = 50$ and respective passband detail; (f) magnitude response for minimax design ($J = N_I$) and respective passband detail. (g) LS optimized bank.

According to the specifications, the prototype filter has order $N_p = (2KM - 1) = 127$. The purpose of the example was to compare different PCLS designs for the same levels of d_1 and d_2. There is also a comparison with designs where the constraint δ_2 is disregarded like in Example 1. As can be observed in Fig. 5, both d_1 and ISI have similar behavior, and d_2 and ICI as well.

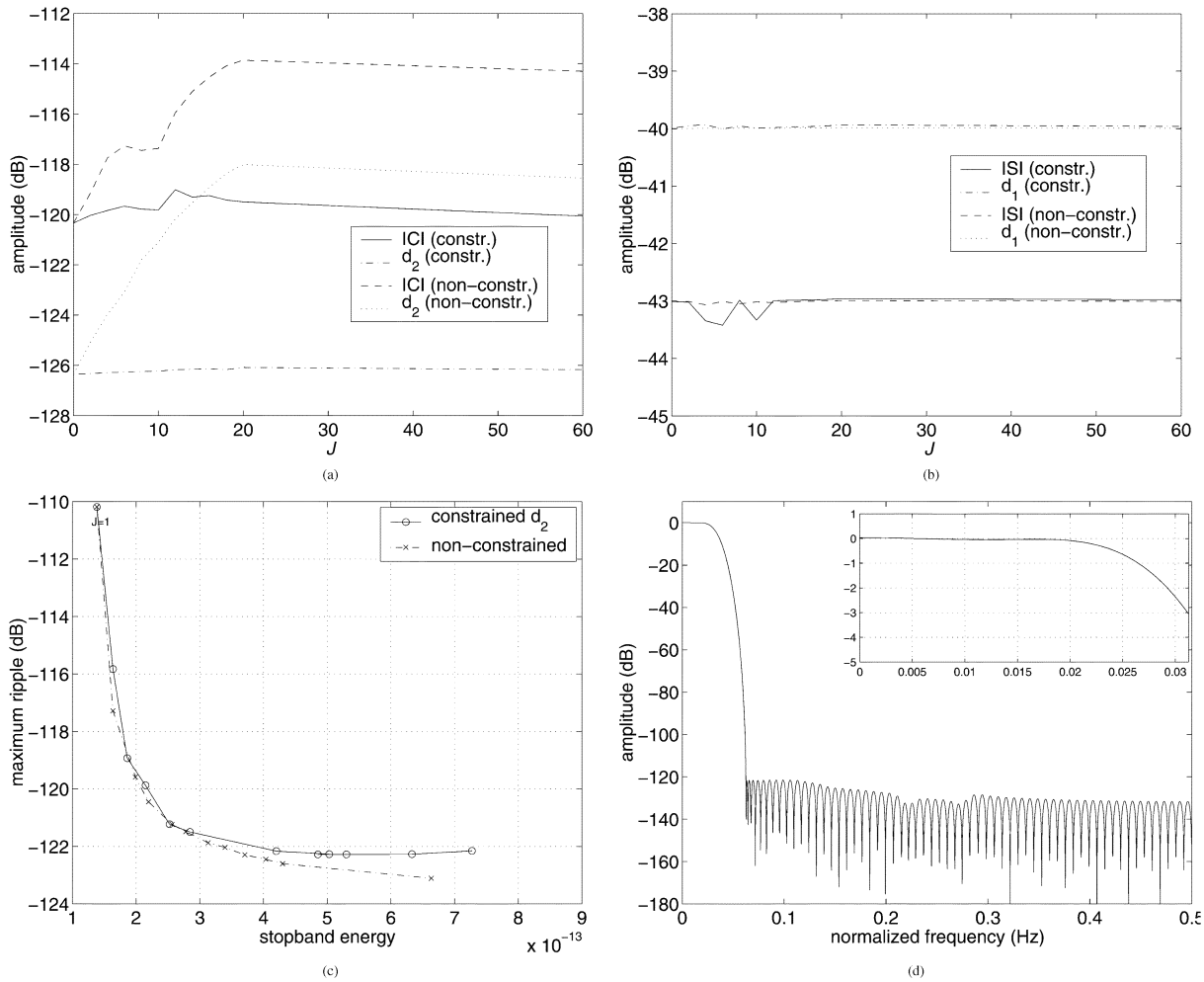

Fig. 5. Example 2 WLS-Chebyshev designs. (a) ICI and d_2 for the constrained d_2 and nonconstrained designs. (b) ISI and d_1 for the constrained d_2 and nonconstrained designs. (c) E_2/E_∞ tradeoff for the d_2 constrained and nonconstrained designs. (d) Magnitude response of prototype filter for $J = 10$ and constrained d_2 with respective passband detail.

The E_2 and E_∞ performances of the constrained d_2 designs were expected to be worse than the nonconstrained ones, as confirmed in Table II and from Fig. 5. One can clearly see that the constraint δ_2 on the aliasing distortion was responsible for increasing the stopband energy (E_2) and maximum stopband ripple (E_∞) in several designs when compared to the nonconstrained d_2 designs. Depending on the application, for the same levels of d_1 and d_2 one may prefer the minimax design if the maximum ripple in the stopband is the most important parameter.

Example 3: Example 3 is shown in Fig. 6. In this example, CMFBTs with a large number of bands and three different PCLS tradeoffs were designed and the computational time was measured to give an idea about the complexity of the proposed algorithm. The design was for 512-band CMFBTs. The specifications were

$$\begin{cases} K = 4 \\ \rho = 1.0 \\ \delta_1 = 0.002 \\ \delta_2 \qquad \text{(as low as possible)} \end{cases} \tag{47}$$

which made this example similar to Example 1 but with higher computational cost.

The figures of merit for this example are listed in Table III. As mentioned before, the code was not optimized for speed since it was run in the Matlab® environment, but the computational time (CT) is still acceptable considering the complexity of the optimization problem. The optimization process takes much longer if the design is not LS $(J \neq 1)$ since it requires iterative designs (see Section IV). In general, the CT is higher for the minimax design. As seen in Table III, the designs simulated were for LS, PCLS and minimax objective functions, which were chosen because they lead, respectively, to the minimal, intermediate and maximal computational costs and are good representatives of the PCLS tradeoff curve.

VII. Conclusion

A new design procedure for optimizing the prototype filter of a CMFBT was presented. This new procedure based on the WLS-Chebyshev algorithm introduced flexibility to the design of CMFBT prototype filters, enabling a tradeoff between stopband energy and maximum attenuation, in a simple and efficient

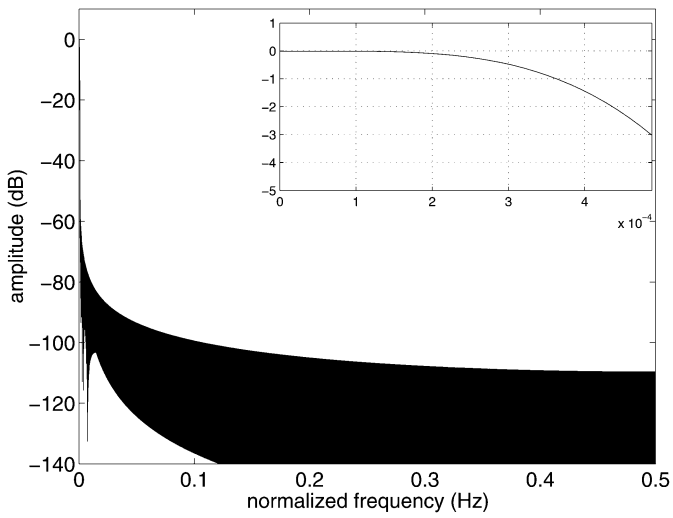

(a)

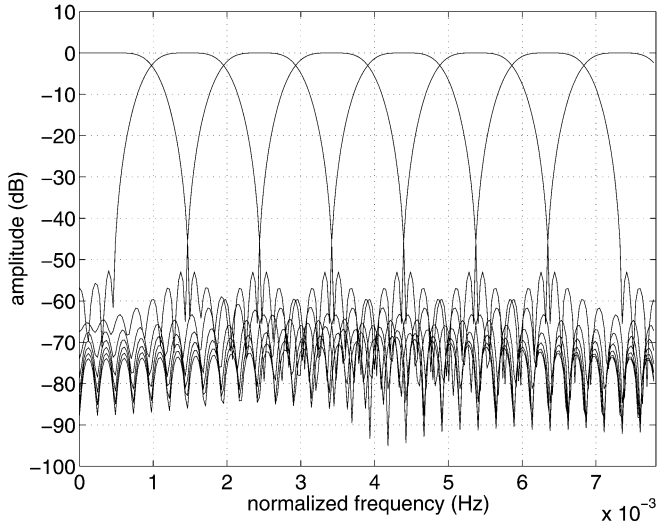

(b)

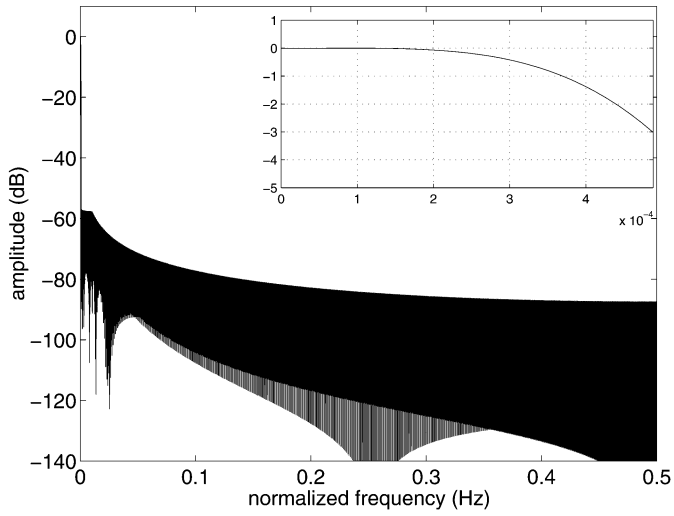

(c)

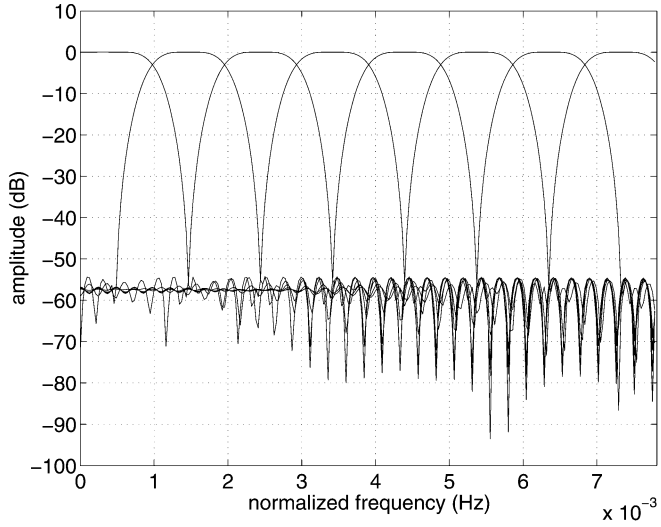

(d)

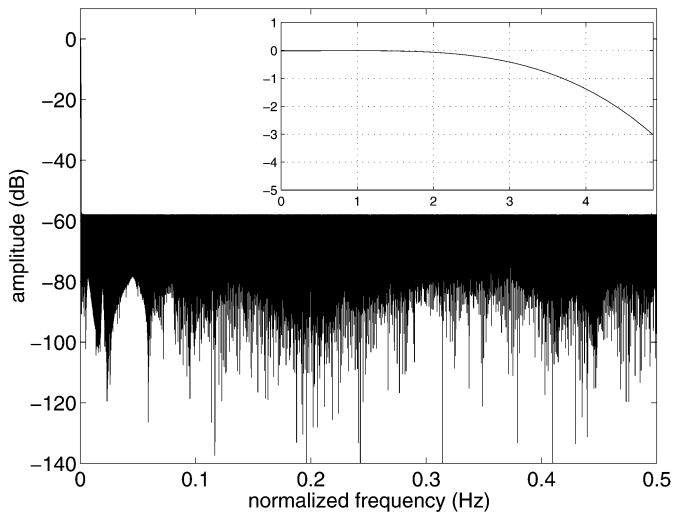

(e)

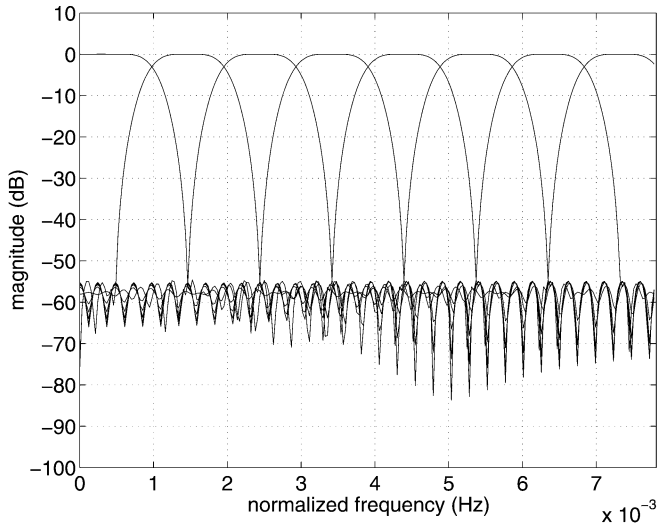

(f)

Fig. 6. Example 3 WLS-Chebyshev designs: (a) Magnitude response of prototype filter for $J = 1$ with respective passband detail. (b) Magnitude response of resulting LS CMFBT bank (8 out of 512 bands). (c) Magnitude response of prototype filter for $J = 40$ with respective passband detail. (d) Magnitude response of resulting PCLS CMFBT bank (8 out of 512 bands). (e) Magnitude response of prototype filter for minimax design with respective passband detail. (f) Magnitude response of resulting minimax CMFBT bank (8 out of 512 bands).

manner. The resulting designs present intermediate levels of ICI or aliasing distortion for a given level of ISI or amplitude distortion. Simulation results had shown that, for an ideal channel, the smaller ICI is achieved by the LS design. From the trans-

TABLE II
FIGURES OF MERIT FOR OPTIMIZED PCLS PROTOTYPE FILTERS IN EXAMPLE 2. CASES $J = 1$ AND $J = N_I = 60$ CORRESPOND TO LS AND MINIMAX DESIGNS, RESPECTIVELY. IN ALL CASES $d_1 = 0.01$ AND $\mathrm{IST} = -43.0$ dB

Figures of Merit	$J = 1$	$J = 10$	$J = 20$	$J = 60$
constrained d_2				
d_2 (dB)	-126.3	-126.2	-126.1	-126.2
E_∞ (dB)	-110.2	-121.5	-122.3	-122.2
E_2 (dB)	1.39×10^{-13}	2.85×10^{-13}	6.33×10^{-13}	7.28×10^{-13}
ICI (dB)	-120.3	-119.8	-119.5	-120.0
non-constrained d_2				
d_2 (dB)	-126.3	-121.8	-118.0	-118.6
E_∞ (dB)	-110.2	-121.5	-122.6	-123.1
E_2 (dB)	1.39×10^{-13}	2.78×10^{-13}	4.30×10^{-13}	6.63×10^{-13}
ICI (dB)	-120.3	-117.4	-113.9	-114.3

TABLE III
FIGURES OF MERIT FOR OPTIMIZED PCLS PROTOTYPE FILTERS IN EXAMPLE 3. CASE $J = 1$ AND $J = N_I = 1022$ CORRESPOND, RESPECTIVELY TO LS AND MINIMAX DESIGNS. IN ALL CASES $d_1 = 0.002$ AND $\mathrm{IST} = -56.0$ dB. CT STANDS FOR COMPUTATIONAL TIME

Figures of Merit	$J = 1$	$J = 40$	$J = N_I$
d_2 (dB)	-54.6	-50.8	-47.8
E_∞ (dB)	-45.5	-56.9	-57.2
E_2 (dB)	9.95×10^{-09}	1.07×10^{-07}	2.17×10^{-06}
ICI (dB)	-51.4	-41.6	-23.6
CT (minutes)	110	350	490

multiplexer point of view, the lowest ICI attainable for a given ISI results in an improved performance of the system, since the reconstructed signal becomes a more accurate copy of the original one.

The proposed WLS-Chebyshev optimization along with the modified objective function evaluated using simplified constraints and gradient vectors are the contributions of this article. They resulted in a flexible PCLS optimization procedure with greatly reduced computational burden.

APPENDIX

Using (4) and (5), (7) can be rewritten as

$$\begin{aligned} T_i(z) = \sum_{m=0}^{M-1} \Big[& \beta_m^{N_p} H_p(z\beta_m) H_p(ze^{-(j2\pi i/M)}\beta_m) \\ & + \beta_m^{-N_p} H_p(z\beta_m^*) H_p(ze^{-(j2\pi i/M)}\beta_m^*) \\ & + {\alpha_m^*}^2 H_p(z\beta_m) H_p(ze^{-(j2\pi i/M)}\beta_m^*) \\ & + {\alpha_m}^2 H_p(z\beta_m^*) H_p(ze^{-(j2\pi i/M)}\beta_m) \Big] \end{aligned}$$

since $({\alpha_m}^2 + {\alpha_m^*}^2) = 0$ and $\alpha_m \alpha_m^* = 1$, for all m. Using (1) and the definition $W_i = e^{(j2\pi i/M)}$, we get

$$\begin{aligned} T_i(z) = & \sum_{n=0}^{2N_p} \left[a_i(n) z^{-n} \sum_{m=0}^{M-1} \left({\beta_m}^{(N_p-n)} + {\beta_m}^{-(N_p-n)} \right) \right] \\ & + \sum_{n=0}^{N_p} \sum_{l=0}^{N_p} \Big[h_p(n) h_p(l) z^{-(n+l)} W_i^l \\ & \times \sum_{m=0}^{M-1} \left({\alpha_m^*}^2 \beta_m^{(n-l)} + {\alpha_m}^2 \beta_m^{-(n-l)} \right) \Big] \end{aligned}$$

where $a_i(n)$ is defined as

$$Z\left\{ (W_i^n h_p(n)) * h_p(n) \right\} = \sum_{n=0}^{2N_p} a_i(n) z^{-n} \tag{48}$$

where $(*)$ denotes linear convolution and $Z\{\cdot\}$ denotes z-transform operations. The following lemma is the key to simplify the optimization problem.

Lemma A.1:

$$\begin{aligned} \gamma(n) &= \sum_{m=0}^{M-1} \left({\beta_m}^{(N_p-n)} + {\beta_m}^{-(N_p-n)} \right) \\ &= \begin{cases} 0, & (N_p - n) \neq 2Mc \\ 2M(-1)^c, & (N_p - n) = 2Mc, c \in \mathbb{Z} \end{cases} \end{aligned} \tag{49}$$

and

$$\begin{aligned} \Gamma(n-l) &= \sum_{m=0}^{M-1} \left({\alpha_m^*}^2 \beta_m^{(n-l)} + {\alpha_m}^2 \beta_m^{-(n-l)} \right) \\ &= \begin{cases} 0, & (n-l) \neq (2c+1)M \\ 2M(-1)^c, & (n-l) = (2c+1)M, c \in \mathbb{Z} \end{cases} \end{aligned} \tag{50}$$

which holds the property $\Gamma(n-l) = -\Gamma(l-n)$.

Proof: Equation (49) is proven in [10], while the general case in (50) follows from rewriting $\Gamma(n-l)$ as [11]

$$\begin{aligned} \Gamma(n-l) = & -je^{(j\pi(n-l)/2M)} \sum_{m=0}^{M-1} (-1)^m e^{(jm\pi(n-l)/M)} \\ & + je^{-(j\pi(n-l)/2M)} \sum_{m=0}^{M-1} (-1)^m e^{-(jm\pi(n-l)/M)} \\ = & -je^{(j\pi(n-l)/2M)} \left[\frac{1 - \left(-e^{(j\pi(n-l)/M)}\right)^M}{1 - \left(-e^{(j\pi(n-l)/M)}\right)} \right] \\ & + je^{-(j\pi(n-l)/2M)} \\ & \times \left[\frac{1 - \left(-e^{-(j\pi(n-l)/M)}\right)^M}{1 - \left(-e^{-(j\pi(n-l)/M)}\right)} \right] \\ = & -\frac{4\cos\frac{\pi(n-l)}{2M} \sin\pi(n-l)}{2\left(1 + \cos\frac{\pi(n-l)}{M}\right)} \\ = & -\frac{\sin\pi(n-l)}{\cos\frac{\pi(n-l)}{2M}}. \end{aligned} \tag{51}$$

■

Using Lemma A.1, then, $T_i(z)$ can be simplified to

$$\begin{aligned} T_i(z) &= \sum_{n=0}^{2N_p} a_i(n) z^{-n} \gamma(n) \\ &\quad + \sum_{n=0}^{N_p} \sum_{l=0}^{N_p} h_p(n) h_p(l) z^{-(n+l)} W_i^l \Gamma(n-l) \\ &= \sum_{n=0}^{2N_p} a_i(n) z^{-n} \gamma(n) \\ &\quad + \sum_{n=0}^{N_p} \sum_{l=n}^{N_p} \Big[h_p(n) h_p(l) z^{-(n+l)} W_i^l \Gamma(n-l) \\ &\quad + h_p(n) h_p(l) z^{-(n+l)} W_i^n \Gamma(l-n) \Big] \\ &= \sum_{n=0}^{2N_p} a_i(n) z^{-n} \gamma(n) \end{aligned} \tag{52}$$

since

$$\begin{aligned} \sum_{n=0}^{N_p} \sum_{l=n}^{N_p} h_p(n) h_p(l) z^{-(n+l)} W_i^l \Gamma(n-l) = \\ - \sum_{n=0}^{N_p} \sum_{l=n}^{N_p} h_p(n) h_p(l) z^{-(n+l)} W_i^n \Gamma(n-l). \end{aligned} \tag{53}$$

In this way, all functions $T_i(z)$ can be evaluated using this simplification, convolving the prototype filter with its complex modulated version, as follows:

$$T_i(z) = Z\left\{ \left(W_i^n h_p(n) * h_p(n) \right) \gamma(n) \right\} \tag{54}$$

for $i = 0, 1, \ldots, (M-1)$. Due to the symmetry in the modulation function, it follows that $T_i(z) = T_{M-i}(z)$. Hence, one may evaluate functions $T_i(z)$ only for $i = 0, 1, \ldots, N_c$. If the prototype filter has a linear phase, then, the functions $T_i(z)$ can be analytically written as

$$\begin{aligned} T_i(z) = z^{-N_p} 2M \Big[a_i(N_p) + \sum_{l=1}^{K-1} a_i(N_p - 2Ml)(-1)^l \\ \cdot \left(z^{2Ml} + z^{-2Ml} \right) \Big] \end{aligned} \tag{55}$$

which is the z-transform of (34).

REFERENCES

[1] J. W. Adams, "FIR digital filters with least-squares stopbands subject to peak-gain constraints," *IEEE Trans. Circuits and Syst.*, vol. 39, no. 4, pp. 376–388, Apr. 1991.

[2] A. N. Akansu, P. Duhamel, L. Xueming, and M. de Courville, "Orthogonal transmultiplexers in communication: A review," *IEEE Trans. Signal. Process.*, vol. 46, no. 4, pp. 979–995, Apr. 1998.

[3] J. Alhava and A. Viholainen, "Coefficient quantization in perfect-reconstruction cosine-modulated filter banks," in *Proc. Eur. Signal Processing Conf.*, Tampere, Finland, Sep. 2000, pp. 1747–1750.

[4] J. A. C. Bingham, "Multicarrier modulation for data transmission: An idea whose time has come," *IEEE Commun. Mag.*, no. 5, pp. 5–14, May 1990.

[5] R. Bregović and T. Saramäki, "Design and properties of two-channel FIR filter banks optimized by using peak-constrained least squares optimization criterion," in *Proc. 2nd Int. Workshop Spectral Methods and Multirate Signal Processing*, Toulouse, France, Sep. 2002, pp. 33–39.

[6] K.-W. Cheong and J. M. Cioffi, "Discrete wavelet transforms in multi-carrier modulation," in *Proc. Global Telecommunications Conf. (GLOBECOM '98)*, vol. 5, Nov. 1998, pp. 2794–2799.

[7] P. S. R. Diniz and S. L. Netto, "On WLS-Chebyshev FIR digital filters," *J. Circuits Syst. Comput.*, vol. 9, no. 3/4, pp. 155–168, 1999.

[8] P. S. R. Diniz, E. A. B. da Silva, and S. L. Netto, *Digital Signal Processing: System Analysis and Design*. Cambridge, U.K.: Cambridge Univ. Press, 2002.

[9] N. J. Fliege, *Multirate Digital Signal Processing*. Chichester, U.K.: Wiley, 1994.

[10] M. B. Furtado, P. S. R. Diniz, and S. L. Netto, "Optimized prototype filter based on the FRM approach for cosine-modulated filter banks," *Circuits Syst. Signal Process.*, vol. 22, no. 2, pp. 193–210, 2003.

[11] ——, "Optimization techniques for cosine-modulated filter banks based on the frequency-response masking approach," in *Proc. IEEE Int. Symp. Circuits and Systems*, Bangkok, Thailand, May 2003.

[12] R. D. Koilpillai and P. P. Vaidyanathan, "Cosine-modulated FIR filter banks satisfying perfect reconstruction," *IEEE Trans. Signal Process.*, vol. 40, no. 4, pp. 770–783, Apr. 1992.

[13] C. L. Lawson, "Contribution to the theory of linear least maximum approximations," Ph.D. dissertation, Univ. of California, Los Angeles, 1961.

[14] Y. C. Lim, J. H. Lee, C. K. Chen, and R. H. Yang, "A weighted least squares algorithm for quasiequiripple FIR and IIR digital filter design," *IEEE Trans. Signal Process.*, vol. 40, no. 3, pp. 551–558, Mar. 1992.

[15] W. S. Lu, "Minimax design of nonlinear-phase FIR filters: A least- P th approach," in *Proc. IEEE Int. Symp. Circuits Systems*, Phoenix, AZ, May 2002, pp. I.409–I.412.

[16] D. G. Luenberger, *Linear and Nonlinear Programming*, 2nd ed. Menlo Park, CA: Addison-Wesley, 1989.

[17] T. Q. Nguyen, "Near-perfect-reconstruction pseudo-QMF banks," *IEEE Trans. Signal Process.*, vol. 42, pp. 65–76, Jan. 1994.

[18] H. S. Malvar, "Extended lapped transforms: Properties, applications, and fast algorithms," *IEEE Trans. Signal Processing*, vol. 40, no. 11, pp. 2703–2714, Nov. 1992.

[19] J. H. McClellan, T. W. Parks, and L. R. Rabiner, "A computer program for designing optimum FIR linear-phase digital filters," *IEEE Trans. Audio Electroacoust.*, vol. AU-21, no. 12, pp. 506–526, Dec. 1973.

[20] A. D. Rizos, J. G. Proakis, and T. Q. Nguyen, "Comparison of DFT and cosine modulated filter banks in multicarrier modulation," in *Global Telecommunications Conf. (GLOBECOM '94)*, vol. 2, Nov.–Dec. 28, 1994, pp. 687–691.

[21] S. D. Sandberg and M. A. Tzannes, "Overlapped discrete multitone modulation for high speed copper wire communications," *IEEE J. Select. Areas Commun.*, vol. 13, no. 9, pp. 1571–1585, Dec. 1995.

[22] T. Saramäki, "A generalized class of cosine-modulated filter banks," in *Proc. TICSP Workshop on Transforms and Filter Banks*, Tampere, Finland, Jun. 1998, pp. 336–365.

[23] P. P. Vaidyanathan, *Multirate Systems and Filter Banks*. Englewood Cliffs, NJ: Prentice-Hall, 1993.

[24] P. P. Vaidyanathan, Y.-P. Lin, S. Akkarakaran, and S.-M. Phoong, "Discrete multitone modulation with principal component filter banks," *IEEE Trans. Circuits Syst.*, vol. 49, no. 10, pp. 1397–1412, Oct. 2002.

[25] A. Viholainen, T. Saramäki, and M. Renfors, "Nearly-perfect reconstruction cosine-modulated filter bank design for VDSL modems," in *Proc. IEEE Int. Conf. Electronics, Circuits, Systems*, Paphos, Greece, Sep. 1999, pp. 373–376.

Miguel B. Furtado, Jr. (S'02) received the B.Sc. degree in electrical engineering and the M.Sc. degree in electrical engineering from the Federal University of Rio de Janeiro (UFRJ), Rio de Janeiro, Brazil, in 2001, and 2002, respectively. He is currently working toward the Ph.D. degree in electrical engineering at UFRJ.

His research interest is in signal processing, communications, and information theory.

Paulo S. R. Diniz (S'80–M'81–SM'92–F'00) was born in Niterói, Brazil. He received the degree in electronics engineering (*cum laude*) and the M.Sc. degree in electrical engineering from the Federal University of Rio de Janeiro (UFRJ), Rio de Janeiro, Brazil, in 1978, and 1981, respectively, and the Ph.D. degree in electrical engineering from Concordia University, Montreal, PQ, Canada, in 1984.

Since 1979, he has been with the Department of Electronic Engineering (the Undergraduate Department), UFRJ. He has also been with the Program of Electrical Engineering (the Graduate Studies Department), UFRJ, since 1984, where he is presently a Professor. He served as an Undergraduate Course Coordinator and as Chairman of the Graduate Department. He is one of the three senior researchers and coordinators of the National Excellence Center in Signal Processing, UFRJ. From January 1991 to July 1992, he was a Visiting Research Associate in the Department of Electrical and Computer Engineering, University of Victoria, Victoria, BC, Canada. He also holds a Docent position at Helsinki University of Technology, Helsinki, Finland. From January 2002 to June 2002, he was a Melchor Chair Professor in the Department of Electrical Engineering, University of Notre Dame, Notre Dame, IN. His teaching and research interests are in analog and digital signal processing, adaptive signal processing, digital communications, wireless communications, multirate systems, stochastic processes, and electronic circuits. He has authored several refereed papers in some of these areas and the books *Adaptive Filtering: Algorithms and Practical Implementation* (Norwell, MA: Kluwer, 2002), and *Digital Signal Processing: System Analysis and Design* with E. A. B. da Silva and S. L. Netto (Cambridge, U.K.: Cambridge Univ. Press, 2002). He has served as an Associate Editor of the *Circuits Syst. Signal Process. Journal* from 1998 to 2002.

Dr. Diniz received the Rio de Janeiro State Scientist Award, from the Governor of Rio de Janeiro state. He was the Technical Program Chair of the 1995 Midwest Symposium on Circuits and Systems (MWSCAS) held in Rio de Janeiro, Brazil. He has been on the Technical Committee of several international conferences including the IEEE International Symposium on Circuits and Systems, the IEEE International Conference on Electronics, Circuits, and Systems, the European Signal Processing Conference, and MWSCAS. He has served as Vice President for Region 9 of the IEEE Circuits and Systems Society (IEEE CAS-S) and as Chairman of the Digital Signal Processing Technical Committee of IEEE CAS-S. He has served as an Associate Editor of the IEEE TRANSACTIONS ON CIRCUITS AND SYSTEMS—II: ANALOG AND DIGITAL SIGNAL PROCESSING from 1996 to 1999, IEEE TRANSACTIONS ON SIGNAL PROCESSING from 1999 to 2002. He was a Distinguished Lecturer of the IEEE CAS-S for the 2000–2001, and the IEEE Signal Processing Society for 2004. He received the 2004 Education Award of the IEEE CAS-S. Dr. Diniz is a Fellow of IEEE *for fundamental contributions to the design and implementation of fixed and adaptive filters and Electrical Engineering Education*.

Sergio L. Netto (SM'04) was born in Rio de Janeiro, Brazil. He received the B.Sc. (*cum laude*) the M.Sc. degrees from the Federal University of Rio de Janeiro (UFRJ) in 1991 and 1992, respectively and the Ph.D. degree from the University of Victoria, Victoria, BC, Canada, in 1996, all in electrical engineering.

Since 1997, he has been an Associate Professor in the Department of Electronics and Computer Engineering, UFRJ, and, since 1998, with the Program of Electrical Engineering, UFRJ. His research interests lie in the fields of digital signal processing, adaptive signal processing, and speech processing. He is the coauthor (with P. S. R. Diniz and E. A. B. da Silva) of *Digital Signal Processing: System Analysis and Design* (Cambridge, U.K.: Cambridge Univ. Press, 2002). He is an Associate Editor of *Circuits Syst. Signal Process.*.

Dr, Netto has served as the Vice-President for Region 9 of the IEEE Circuits and Systems Society in 2002 and 2003.